Supramolecular Chemistry
Publication details, including instructions for authors and subscription information:
http://www.informaworld.com/smpp/title~content=t713649759

Construction of acetate-bridged dicopper(II) hybrid organic-inorganic networks with calix[4]arene-derived nitrogenous ligands

Juan Olguín[a]; Adrián Castillo[a]; Virginia Gómez-Vidales[a]; Simón Hernández-Ortega[a]; Rubén A. Toscano[a]; Eduardo Muñoz[b]; Ivan Castillo[a]
[a] Instituto de Química, Universidad Nacional Autónoma de México, Circuito Exterior, Ciudad Universitaria, México, DF, Mexico [b] Instituto de Física, Universidad Nacional Autónoma de México, Circuito Exterior, Ciudad Universitaria, México, DF, Mexico

To cite this Article Olguín, Juan , Castillo, Adrián , Gómez-Vidales, Virginia , Hernández-Ortega, Simón , Toscano, Rubén A. , Muñoz, Eduardo and Castillo, Ivan(2009) 'Construction of acetate-bridged dicopper(II) hybrid organic-inorganic networks with calix[4]arene-derived nitrogenous ligands', Supramolecular Chemistry, 21: 6, 502 — 509
To link to this Article: DOI: 10.1080/10610270802406561
URL: http://dx.doi.org/10.1080/10610270802406561

Supramolecular Chemistry
Vol. 21, No. 6, September 2009, 502–509

Taylor & Francis
Taylor & Francis Group

Construction of acetate-bridged dicopper(II) hybrid organic–inorganic networks with calix[4]arene-derived nitrogenous ligands

Juan Olguín[a], Adrián Castillo[a], Virginia Gómez-Vidales[a], Simón Hernández-Ortega[a], Rubén A. Toscano[a], Eduardo Muñoz[b] and Ivan Castillo[a]*

[a]*Instituto de Química, Universidad Nacional Autónoma de México, Circuito Exterior, Ciudad Universitaria, México, DF, Mexico;*
[b]*Instituto de Física, Universidad Nacional Autónoma de México, Circuito Exterior, Ciudad Universitaria, México, DF, Mexico*

(*Received 17 April 2008; final version received 29 July 2008*)

The reactions of mono-, bis- and tetrapicolyl-*p-tert*-butylcalix[4]arene derivatives functionalised in the phenolic positions ($\mathbf{L^1}$–$\mathbf{L^4}$) with copper(II) acetate resulted in the formation of discrete complexes or extended coordination polymers. The centrosymmetric dimer $[Cu_2(\mu\text{-}O_2CCH_3)_4(\mathbf{L^1})_2]$ **1**, obtained with monodentate $\mathbf{L^1}$, has square pyramidal coordination around the copper centres and a cone conformer of monopicolyl-calix[4]arene acting as an axial ligand, with a molecule of acetonitrile hosted within its cavity. The potentially bidentate $\mathbf{L^2}$ acts as a monodentate ligand, affording the complex $[Cu_2(\mu\text{-}O_2CCH_3)_4(\mathbf{L^2})_2]$ **2**, which based on spectroscopic and combustion analysis data has a similar coordination sphere around Cu(II). Compound $\mathbf{L^3}$ bridges two dicopper units in the coordination polymer $[Cu_2(\mu\text{-}O_2CCH_3)_4(\mu\text{-}\mathbf{L^3})]_n$ **3**, with the calixarene hosting a molecule of tetrahydrofuran. Finally, compound $\mathbf{L^4}$ reacts with 4 equivalents of copper(II) acetate, presumably generating a two-dimensional coordination polymer formulated as $[\{Cu_2(\mu\text{-}O_2CCH_3)_4\}_2(\mathbf{L^4})]$ **4**.

Keywords: calixarenes; copper; crystal structure; hybrid material

Introduction

The macrocycles known as calixarenes have been the subject of intensive research in the field of supramolecular chemistry due to their versatility as host molecules, preorganised structure and the ease of modification with several functional groups (*1*, *2*). The latter property has allowed the introduction of donor groups for the preparation of transition metal complexes with different metal–element (M–E) bonds (E = N, O, P, S) (*3–5*). In addition, the well-defined geometry of the calixarene derivatives has resulted in the development of novel building blocks for the construction of molecular networks (*6*). The combination of both properties of calixarene derivatives, to act as ligands towards transition metals, and to act as building blocks in the construction of extended networks, represents an attractive option for the assembly of hybrid organic–inorganic materials.

Among the functional groups that have been incorporated into calixarenes, nitrogen-containing heterocycles represent an important class due to their donor properties towards transition metals, with examples reported of picolyl (*7*), imidazolyl (*8*), bipyridyl (*9*) and phenantroyl functionalities (*10*). In the specific case of *p-tert*-butylcalix[4]arene, the bispicolyl derivative substituted in alternate phenolic positions has allowed us to prepare a hybrid organic–inorganic coordination polymer of dimeric Cu(II) paddle-wheel units with bridging acetate ligands ($\mathbf{L^3}$ in Scheme 1, R = H) (*11*). Despite the existence of reports of d-block metal complexes with related picolyl-substituted calix[4]arenes ($\mathbf{L^3}$, R = methyl or *n*-butyl) (*8*, *12*), which feature non-coordinating anions, such as PF_6^-, ClO_4^- and NO_3^-, the acetate-bridged linear polymer represents the only example of this class of compounds which has been structurally characterised to date. To determine the capability of various picolyl-substituted *p-tert*-butylcalix[4]arenes as organic connectors in the assembly of hybrid organic–inorganic networks, we herein report the preparation, spectroscopic properties and solid-state structures of Cu(II) acetate complexes with the *p-tert*-butylcalix[4]arene derivatives $\mathbf{L^1}$–$\mathbf{L^4}$ (Scheme 1, R = H) (*13–16*).

Results and discussion

Our approach for the synthesis of Cu(II) complexes involves the use of the dimeric paddle-wheel unit $Cu_2(\mu\text{-}O_2CR)_4$, which has proved effective as a linear connector in hybrid metal–organic frameworks with intricate architectures (*17*). Thus, mixing the appropriate number of equivalents of the ligands $\mathbf{L^1}$–$\mathbf{L^4}$ with copper(II) acetate in a suitable solvent mixture afforded the corresponding complexes **1**–**4** in good yields as turquoise crystalline solids. Initial characterisation was accomplished by IR spectroscopy measured on KBr pellets (Figure 1).

*Corresponding author. Email: joseivan@servidor.unam.mx

ISSN 1061-0278 print/ISSN 1029-0478 online

DOI: 10.1080/10610270802406561
http://www.informaworld.com

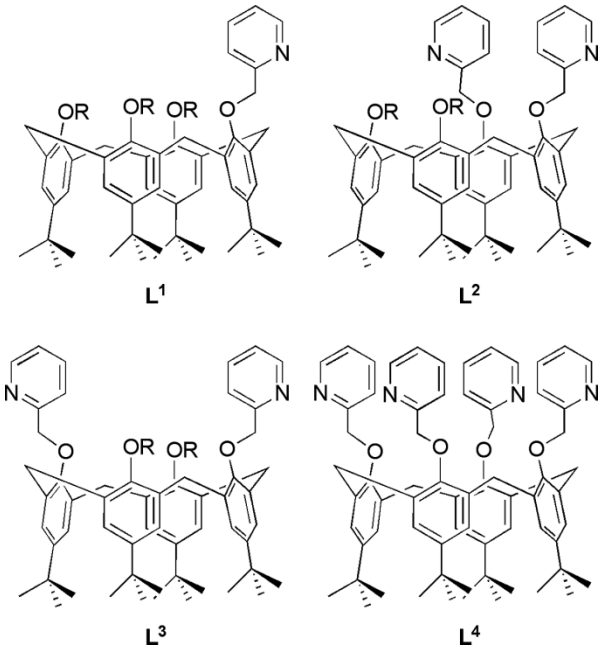

Scheme 1. *p-Tert*-butylcalix[4]arene derivatives $\mathbf{L^1}$–$\mathbf{L^4}$.

The spectra obtained exhibit strong absorptions at 3287–3411 cm^{-1} due to the ν(OH) of the intramolecularly hydrogen-bonded calixarene-derived ligands in complexes **1**–**3**, while the fingerprint region in all spectra confirms the presence of the aromatic groups of the calixarenes (*18*). In addition, there are strong bands for symmetric and asymmetric $\nu(CO_2)$ of the acetate groups at 1436 and 1620 cm^{-1} for **1**, 1433 and 1627 cm^{-1} for **2**, 1434 and 1625 cm^{-1} for **3** and 1435 and 1624 cm^{-1} for **4**, respectively. The frequency difference between the $\nu(CO_2)$ stretching modes ($\Delta = 184$, 194, 191 and 189 cm^{-1}) is within the range observed for other complexes with bridging acetate ligands (*19*), thus confirming the presence of the dimeric $Cu_2(\mu\text{-}O_2CCH_3)_4$ units.

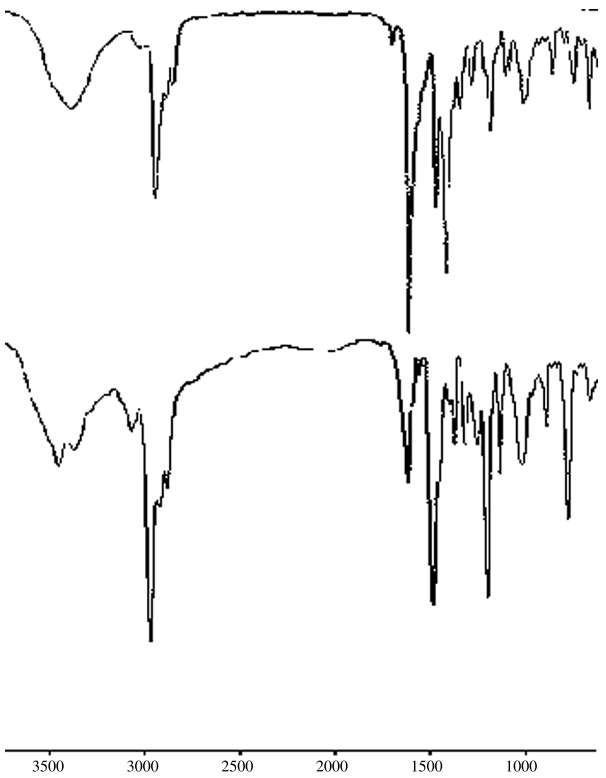

Figure 1. Infrared spectra of **3** and **4** in the 3750–600 cm^{-1} range.

Combustion analysis of the complexes reveals that **1** and **2** possess two calix[4]arene-based ligands per dicopper unit, as well as solvent molecules of crystallisation, consistent with the empirical formulae $[Cu_2(\mu\text{-}O_2CCH_3)_4(\mathbf{L^1})_2]\cdot 3CH_3CN\cdot 2H_2O$ and $[Cu_2(\mu\text{-}O_2CCH_3)_4(\mathbf{L^2})_2]\cdot 2CH_3CN$, respectively. Complexes **1** and **2** were the only products obtained in the reactions of $\mathbf{L^1}$ and $\mathbf{L^2}$ with copper(II) acetate, regardless of the amount of Cu(II) employed. By contrast, the stoichiometry of **3** corresponds to a 1:1 ligand/$Cu_2(\mu\text{-}O_2CCH_3)_4$ ratio, formulated as $[Cu_2(\mu\text{-}O_2CCH_3)_4(\mathbf{L^3})]\cdot H_2O$. Finally, combustion analysis of **4** is consistent with the presence of four copper(II) ions per ligand, consistent with the formula $[\{Cu_2(\mu\text{-}O_2CCH_3)_4\}_2(\mathbf{L^4})]$.

ESR spectroscopic studies

Analysis of the complexes by ESR spectroscopy at X-band frequency confirmed the presence of dimeric copper(II) species in all cases. The spectra obtained at ambient temperature from powder samples correspond to well-resolved triplets ($S = 1$, Figure 2) with axial symmetry and relatively high D values, and were modelled with the spin Hamiltonian in Equation (1) ($D \neq 0$, and $E \approx 0$).

$$H = \beta H_g S + D\left[S_z^2 - 2/3\right] + \left[S_x^2 - S_y^2\right]E. \qquad (1)$$

The parameters obtained (Table 1), which are in good agreement with those reported for analogous systems

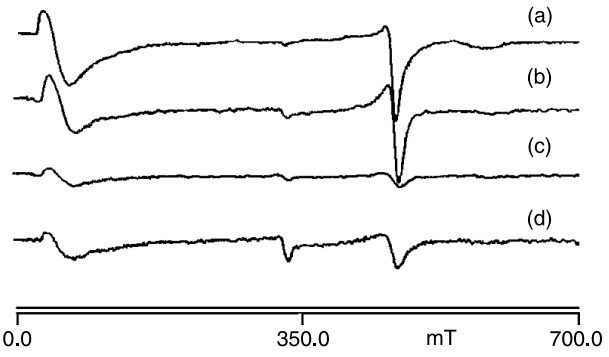

Figure 2. ESR spectra of solid samples (a) **1**, (b) **2**, (c) **3** and (d) **4**; $\upsilon = 9.44$ GHz.

Table 1. Spin Hamiltonian parameters obtained from powder ESR samples.

Compound	H_{z1} (mT)	H_{z2} (mT)	$H_{\perp 2}$ (mT)	$g_{\parallel}$	D (cm^{-1})	D_{dd} (cm^{-1})	$\lvert J\rvert$ (cm^{-1})
1	43.54	586.05	465.8	2.14	0.29	0.16	346
2	54.83	596.23	467.2	2.07	0.27	–	–
3	49.48	588.71	464.17	2.11	0.28	0.16	426
4	40.89	604.68	462.3	2.08	0.29	–	–

(*20*), were calculated by taking into account Equations (2) and (3) (*21*).

$$H_{z1} = (g_e/g_{\parallel})(H_o - D'), \quad (2)$$

$$H_{z2} = (g_e/g_{\parallel})(H_o + D'), \quad (3)$$

where $D' = D/\beta g_e$, $g_e = 2.0023$ and $H_o = h\nu/g_e\beta$. The experimental D value is the sum of two contributions to the observed zero-field splitting of the spin triplet. One of them arises from the dipole–dipole interaction between the unpaired spins in the two copper centres. The other one is provided by the so-called anisotropic exchange, and arises from the spin–orbit interaction. The net resultant dipolar part is given by the relationship in Equation (4).

$$D(\exp) = D_{ex} + D_{dd}. \quad (4)$$

The exchange and dipole–dipole interactions were estimated from the relationships in Equations (5) and (6) (*22*, *23*).

$$D_{ex} = -J/8\left[(1/4)(g_{\parallel} - 2)^2 - (g_{\perp} - 2)^2\right], \quad (5)$$

$$D_{dd} = -(g_{\parallel}^2 + 1/2g_{\perp}^2)(\beta^2/r^3). \quad (6)$$

Below 77 K, the spectra collapse to a single resonance due to a dilute paramagnetic impurity ($S = 1/2$). These observations are consistent with strongly antiferromagnetically coupled Cu(II) centres. Based on the distance between copper(II) ions in the solid-state structures obtained (r in Equation (6)), it was possible to derive values for the coupling constants of $J = -346\,cm^{-1}$ for **1** and $-426\,cm^{-1}$ for **3**.

Solid-state structures of 1 and 3

Single crystals of **1** were obtained by slow evaporation of a concentrated acetonitrile solution. The solid-state structure (triclinic space group $P-1$, Table 2) confirmed that the symmetry-related copper(II) centres in **1** have a square pyramidal coordination geometry. The base of the pyramid is defined by the four bridging acetates at an average Cu–O bond length of 1.964(4) Å, while the picolyl group acts as a capping axial ligand with a Cu–N bond length of 2.198(4) Å. The distance between the two symmetry-related copper ions is 2.637(1) Å (Table 3 and Figure 3). Two of the four molecules of acetonitrile present in the structure of the centrosymmetric dimer **1**·4CH_3CN are hosted in the calix[4]arene cavities (the ones containing N2 and symmetry-related N2A), which adopt a cone conformation. Inclusion of neutral species within calixarene cavities is a common occurrence (*24*), with several cases reported for acetonitrile molecules (*25*). Within a molecule of dimeric **1**, the calixarene cavities are oriented in opposite directions. In the extended structure, such cavities align forming acetonitrile-filled channels along the direction of the *b*-axis (Figure 4).

The included acetonitrile molecule has two short C56—H$\cdots\pi$ contacts from H56A and H56B to the adjacent phenolic groups, with calculated H$\cdots$centroid distances of 2.819 and 2.719 Å, respectively. The corresponding C—H$\cdots$centroid angles are 163.81 and 148.91°. In addition, there are two longer C–H56C contacts to the other two phenolic π clouds (3.097 Å and 122.57° to the picolyl-containing phenoxy moiety, and 3.079 Å and 124.81° to the remaining phenolic group).

Reactions of $\mathbf{L^2}$ with 1–2 equivalents of copper(II) resulted invariably in the formation of complex **2**. Attempts to obtain X-ray quality crystals were unsuccessful, but its good solubility in acetonitrile, dichloromethane and chloroform is indicative of a discrete molecular species. Based on the spectroscopic evidence and combustion analysis, it is reasonable to postulate a dimeric structure similar to that of **1**. Since the nitrogen donors are located in adjacent phenolic positions, coordination of a dicopper motif by one of the picolyl groups of $\mathbf{L^2}$ as an axial ligand could result in a complex that is too sterically demanding to accommodate a second picolyl–$Cu_2(\mu\text{-}O_2CCH_3)_4$ interaction, rendering $\mathbf{L^2}$ as a monodentate ligand in this system.

In the case of **3**, its insolubility in common organic solvents (benzene, toluene, acetonitrile, dichloromethane and chloroform), together with a 1:1 ratio of $\mathbf{L^3}$ and $Cu_2(\mu\text{-}O_2CCH_3)_4$ determined by combustion analysis, indicated that its structure must consist of aggregates. Fortunately, slow evaporation of a solution of $\mathbf{L^3}$ and 2 equivalents of copper(II) in THF resulted in the formation of X-ray quality crystals. Data collected at 173 K in the triclinic space group $P-1$ reveal that the coordination environment of the Cu(II) centres is virtually identical to that of **1**, with an average bond length of Cu–O 1.964(2) Å, Cu1–N1 2.267(2) Å, Cu2–N2 2.220(2) Å and a Cu1$\cdots$Cu2 distance

Table 2. Crystallographic data for **1**·4CH_3CN and **3**·2.5C_4H_8O.

	1·4CH_3CN	**3**·2.5C_4H_8O
Formula	$C_{116}H_{146}Cu_2N_6O_{16}$	$C_{148}H_{196}Cu_4N_4O_{29}$
M	2007.47	2749.38
Crystal colour, habit	Turquoise, prism	Turquoise, prism
Crystal size (mm)	0.36 × 0.30 × 0.10	0.18 × 0.25 × 0.28
Crystal system	Triclinic	Triclinic
Space group	$P-1$	$P-1$
a (Å)	12.599(1)	14.013(4)
b (Å)	14.151(1)	14.173(4)
c (Å)	17.666(1)	19.940(5)
α (°)	68.686(1)	109.89(2)
β (°)	76.872(1)	99.89(2)
γ (°)	83.526(1)	91.33(2)
V (Å^3)	2855.9(3)	3654.4(17)
hkl ranges	$-14 \le h \le 14$	$-16 \le h \le 16$
	$-16 \le k \le 16$	$-17 \le k \le 17$
	$-20 \le l \le 21$	$-24 \le l \le 24$
Z	1	1
D_c (g ml^{-1})	1.167	1.249
F (000)	1070	1460
μ (Mo-Kα) (mm^{-1})	0.435	0.645
θ range (°)	1.62–25.00	1.48–25.40
Unique reflections	10,040	13,383
Reflections ($I > 2\sigma(I)$)	4987	8971
No. of refined parameters	725	1143
R_{int}	0.0648	0.0545
Final *R* (*R*′)	0.0749 (0.1549)	0.0487 (0.1231)
Goodness of fit	0.940	0.945
Maximum/minimum peaks in final difference map (e Å^{-3})	0.840, −0.365	1.064, −0.352

of 2.647(1) Å (Table 3 and Figure 5). Nonetheless, the extended structure of **3** differs significantly from that of dimeric **1**. Translation of the asymmetric unit along the *b*-axis generates polymeric chains of **3**·2.5THF, with $\mathbf{L}^3$ acting as a ditopic linker (Figure 6). The structure of **3** is similar to the related pyridine-substituted resorcinarene–copper(II) acetate coordination polymer (*26*). Within a chain of **3**, the calix[4]arene units adopt a *syn* conformation, orienting all the *tert*-butyl groups parallel to the crystallographic *b*-axis. The asymmetric unit contains 2.5 molecules of THF per linear connector $Cu_2(\mu\text{-}O_2CCH_3)_4$, 1.5 of which correspond to *exo*-calixarene solvent molecules that reside near the bridging carboxylate groups. The other equivalent of THF, which contains O13, is hosted within the calix[4]arene. This oxygen atom is oriented away from the cavity, thus allowing C—H···π interactions of the methylene groups of THF with the aromatic rings of the macrocycle. Hydrogen atoms H67A and H67B on C67 have the shortest contacts to the π systems of the picolyl-bearing phenolic rings, with calculated C—H···centroid distances of 2.615 and 2.631 Å and angles of 163.90° and 165.32°. The hydrogen atoms on the adjacent C66 and C68 atoms, located on the same molecule of THF, have longer C—H···π contacts to the unfunctionalised phenolic rings. The corresponding distances to the ring centroids are 3.430 and 3.306 Å for H66A and H66B, and 3.352 and 2.937 for H68A and H68B.

Table 3. Selected bond lengths (Å) and angles (°) for **1**·4CH_3CN and **3**·2.5C_4H_8O.

1·4CH_3CN			
Cu–O5	1.947(3)	O5–Cu–O6	167.65(1)
Cu–O6	1.967(3)	O5–Cu–O7	89.38(2)
Cu–O7	1.978(4)	O5–Cu–O8	90.33(2)
Cu–O8	1.963(4)	O6–Cu–O7	88.23(2)
Cu–N	2.198(4)	O6–Cu–O8	89.37(2)
		O7–Cu–O8	167.42(1)
		N–Cu–Cu	176.64(1)
3·2.5C_4H_8O			
Cu1–O5	1.986(2)	O5–Cu1–O7	88.3(1)
Cu1–O7	1.957(2)	O5–Cu1–O9	164.0(1)
Cu1–O9	1.975(2)	O5–Cu1–O11	88.0(1)
Cu1–O11	1.950(2)	O7–Cu1–O9	90.3(1)
Cu1–N1	2.267(2)	O7–Cu1–O11	169.1(1)
Cu2–O6	1.950(2)	O9–Cu1–O11	90.5(1)
Cu2–O8	1.982(2)	N1–Cu1–Cu2	173.4(1)
Cu2–O10	1.948(2)	O6–Cu2–O8	88.4(1)
Cu2–O12	1.967(2)	O6–Cu2–O10	169.8(1)
Cu2–N12	2.220(2)	O6–Cu2–O12	88.7(1)
		O8–Cu2–O10	90.2(1)
		O8–Cu2–O12	164.6(1)
		O10–Cu2–O12	90.0(1)
		N2–Cu2–Cu1	175.9(1)

Desolvation of **3**·2.5THF upon warming results in the loss of 1.5 molecules of THF per asymmetric unit, resulting in the previously reported **3**·THF, whose structure

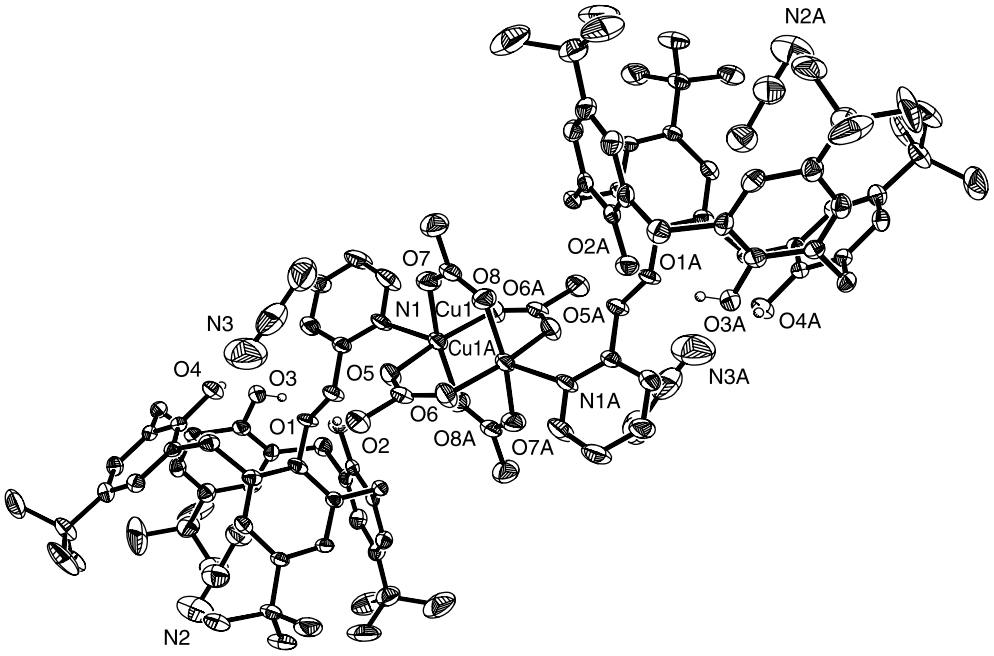

Figure 3. ORTEP diagram of **1**·4CH_3CN showing the non-H-atom displacement ellipsoids at the 30% probability level.

was determined at 294 K (*11*). This single-crystal-to-single-crystal transformation is accompanied by an expansion of the unit cell, as evidenced in the corresponding volumes of 3654.4(17) and 3709.2(17) $Å^3$. The higher THF content of the single crystals of **3**·2.5THF correspond to a calculated density of 1.249 g ml^{-1}, while that of **3**·THF is 1.134 g ml^{-1}. The crystals are characterised by the presence of solvent accessible voids of 101 and 292 $Å^3$ per unit cell, respectively, which together with the loss of THF molecules upon warming indicate the capability of these hybrid materials to allow the mobility of guests despite the absence of pores (*27*).

As in the case of **3**, complex **4** is insoluble in common organic solvents, consistent with an extended structure. Combustion analysis of **4** indicates the binding of two $Cu_2(\mu\text{-}O_2CCH_3)_4$ motifs per ligand, which would result in a two-dimensional coordination polymer with Cu–N interactions in all four picolyl groups of $\mathbf{L}^4$. Unfortunately, the solid-state structure of **4** was not determined. The complex is only sparingly soluble in strongly coordinating solvents (dimethyl sulphoxide, dimethylformamide, dioxane and THF), probably due to the formation of $Cu_2(\mu\text{-}O_2CCH_3)_4$ solvates dissociated from $\mathbf{L}^4$, which upon evaporation of the solvents resulted in the formation of microcrystals of **4** that were not suitable for single-crystal structure determination.

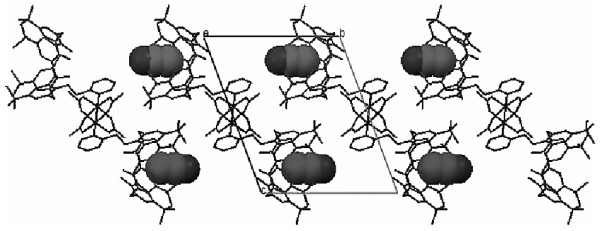

Figure 4. Crystal packing of **1**·4CH_3CN with aligned molecules of acetonitrile forming pseudo-channels.

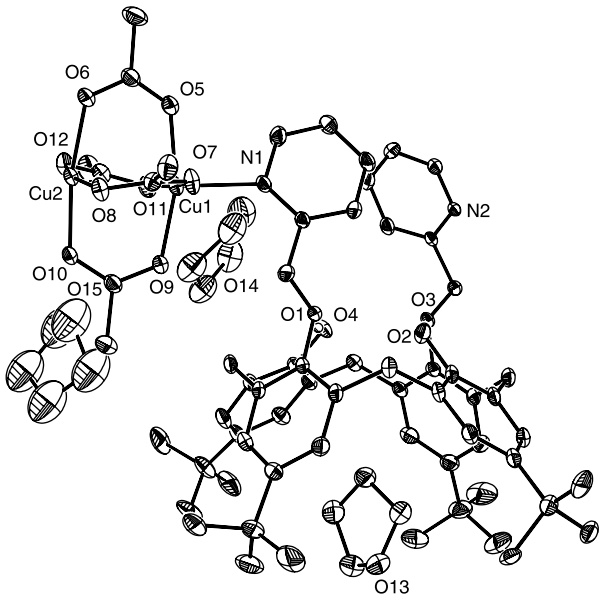

Figure 5. ORTEP diagram of the asymmetric unit of **3**·2.5THF at 173 K, the molecule of tetrahydrofuran which contains O15 sits at a special position.

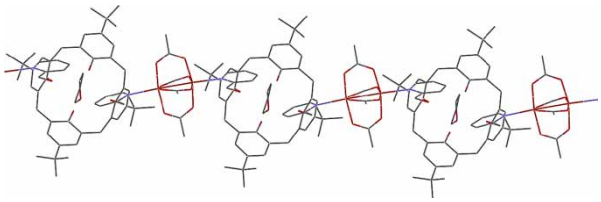

Figure 6. Stick representation of the linear polymer **3**·2.5THF along the *b*-axis with molecules of tetrahydrofuran inside the calix[4]arene cavities.

Based on the IR and ESR data, it is clear that the structure of the linear paddle-wheel connector $Cu_2(\mu\text{-}O_2CCH_3)_4$ is maintained upon interaction with the picolyl-substituted *p-tert*-butylcalix[4]arenes. This was confirmed in the solid-state structure of the molecular complex **1**, which constitutes the starting point for building networks of increasing dimensionality. In this context, compounds $\mathbf{L^2}$ and $\mathbf{L^3}$ represent potential building blocks for zigzag and linear coordination polymers, respectively. The adjacent position of the picolyl substituents in $\mathbf{L^2}$ appears to preclude the formation of either a coordination polymer, or cyclic oligomers, all of which require a 1:2 $\mathbf{L^2}$/copper(II) stoichiometry. Instead, complex **2** with 1:1 stoichiometry (two ligands per $Cu_2(\mu\text{-}O_2CCH_3)_4$ linker) was obtained. In the case of $\mathbf{L^3}$, the expected linear coordination polymer **3** was obtained. This complex undergoes a single-crystal-to-single-crystal transformation upon desolvation, as determined by comparison with previously reported results (*11*). Although $\mathbf{L^4}$ has adjacent picolyl groups, combustion analysis of the copper complex **4** indicates that every picolyl moiety interacts with a $Cu_2(\mu\text{-}O_2CCH_3)_4$ linker, which is consistent with a two-dimensional coordination polymer. This behaviour contrasts with that of $\mathbf{L^2}$, which acts as a monodentate ligand, and can be attributed to a cooperative effect in the formation of four Cu–N bonds in complex **4**, thus overcoming the steric hindrance exerted by the adjacent dicopper connectors.

Conclusions

In summary, we have demonstrated that *p-tert*-butylcalix[4]arene ligands functionalised with picolyl groups are useful building blocks for the construction of novel hybrid organic–inorganic polymers with dicopper connectors. In these systems, $\mathbf{L^1}$ can be employed as a capping, monodentate ligand for the dimeric copper(II) acetate. Of the potentially bidentate pro-ligands $\mathbf{L^2}$ and $\mathbf{L^3}$, the substitution pattern of the former in the adjacent phenolic positions appears to prevent coordination of one of the picolyl groups, rendering $\mathbf{L^2}$ as a formally monodentate ligand. Thus, only $\mathbf{L^3}$ favours the formation of linear chains by acting as bridging bidentate ligand, linking two $Cu_2(\mu\text{-}O_2CCH_3)_4$ units. In contrast to the behaviour of $\mathbf{L^2}$, combustion analysis of **4** appears to indicate that every picolyl group of $\mathbf{L^4}$ interacts with $Cu_2(\mu\text{-}O_2CCH_3)_4$ linkers, presumably acting as a bridging ligand analogous to $\mathbf{L^3}$, giving rise to a two-dimensional coordination polymer. Based on the previous observations when other copper salts are employed in the synthesis of related complexes (*8*, *12*), the presence of acetate ligands in the coordination sphere of the Cu(II) ions appears to be crucial for the formation of crystalline products. Further studies with Cu(II) salts featuring different coordinating anions, i.e. $CuCl_2$ and $CuBr_2$, are necessary to assess the possibility of preparing analogous organic–inorganic hybrids with monocopper linkers.

Experimental

General

Solvents and reagents were obtained from commercial suppliers and used without further purification. The ligands employed $\mathbf{L^1}$–$\mathbf{L^4}$ were prepared by slight modification of the literature procedures (*13–16*). Infrared spectra were obtained with a Perkin-Elmer 203-B spectrometer in the range of 4000–400 cm^{-1} as KBr disks, and UV–vis spectra on a Shimadzu UV-160U spectrophotometer as acetonitrile (**1** and **2**) or tetrahydrofuran (THF, **3** and **4**) solutions. Combustion analyses were performed by Galbraith Laboratories, Knoxville, TN, USA.

Synthesis of $[Cu_2(\mu\text{-}O_2CCH_3)_4(L^1)_2]$ *1*

Compound $\mathbf{L^1}$ (0.20 g, 0.27 mmol) was dissolved in 10 ml of a 1:1 chloroform/acetonitrile mixture. A solution of copper(II) acetate (0.05 g, 0.27 mmol) in 5 ml of acetonitrile was added dropwise while stirring, resulting in a colour change from blue to green. After the addition was completed, the mixture was filtered, and the solvents were allowed to evaporate until green crystals of **1** were formed. The product was isolated by filtration, and further evaporation of the mother liquor resulted in the formation of more crystals of **1** for a total isolated yield of 75% (0.17 g, 0.10 mmol). Single crystals for X-ray diffraction were obtained by slow evaporation of an acetonitrile solution of **1**. Anal. calcd for $C_{114}H_{147}N_5O_{18}Cu_2$ (**1**·$3CH_3CN$·$2H_2O$): C 68.38, H 7.40, N 3.50. Found: C 68.02, H 7.34, N 3.30%. IR (KBr, cm^{-1}): ν = 3287, 2946, 2907, 2871, 1620, 1485, 1436, 1394, 1385, 1298, 1204, 1125, 1104, 1024, 1010, 946. UV–vis [λ_{max}, nm (ε, 1 mol^{-1} cm^{-1})]: (CH_3CN solution) 672 (575).

Synthesis of $[Cu_2(\mu\text{-}O_2CCH_3)_4(L^2)_2]$ *2*

To a solution of $\mathbf{L^2}$ (0.05 g, 0.06 mmol) in 5 ml of a 1:1 chloroform/acetonitrile mixture was added dropwise and with stirring a solution of copper(II) acetate (0.01 g,

0.06 mmol) in 5 ml of acetonitrile. During the addition, the colour of the mixture changed from blue to green. After the addition was complete, the volatile materials were distilled, and green microcrystals of **2** were obtained. The product was washed with distilled water and hot hexanes, and after drying under vacuum a 69% yield was recovered (0.04 g, 0.02 mmol). Anal. calcd for $C_{124}H_{150}N_6O_{16}Cu_2$ (**2**·2CH_3CN): C 70.66, H 7.17, N 3.99. Found: C 70.68, H 7.28, N 3.66%. IR (KBr, cm^{-1}): $\nu = 3324, 2956, 2869, 1714, 1627, 1484, 1433, 1388, 1364, 1297, 1246, 1200, 1126, 1031, 947, 871, 762, 681, 627$. UV–vis [$\lambda_{max}$, nm ($\varepsilon$, $l\,mol^{-1}\,cm^{-1}$)]: (CH_3CN solution) 673 (533).

Synthesis of $[Cu_2(\mu\text{-}O_2CCH_3)_4(\mu\text{-}L^3)]_n$ *3*

Compound $\mathbf{L^3}$ was dissolved in 5 ml of acetonitrile (0.06 g, 0.07 mmol), and a solution of copper(II) acetate (0.01 g, 0.14 mmol) in 5 ml of acetonitrile was added dropwise while stirring. During the addition, the mixture turned deep green. When the addition of copper(II) acetate was complete, a green solid started to deposit. The microcrystals obtained in this manner were washed with distilled water, followed by hot hexanes, for a 91% yield of **3** (0.04 g, 0.03 mmol). Single crystals for X-ray diffraction were obtained by slow evaporation of a THF solution of **3**. Anal. calcd for $C_{64}H_{80}N_2O_{13}Cu_2$ (**3**·H_2O): C 63.40, H 6.65, N 2.31. Found: C 63.51, H 6.85, N 2.34%. IR (KBr, cm^{-1}): $\nu = 3411, 2959, 2908, 2869, 1717, 1625, 1484, 1434, 1383, 1300, 1189, 1124, 1102, 1028, 873, 762, 683, 626$. UV–vis [$\lambda_{max}$, nm ($\varepsilon$, $l\,mol^{-1}\,cm^{-1}$)]: (THF solution) 670 (300).

Synthesis of $[Cu_2(\mu\text{-}O_2CCH_3)_4(\mu\text{-}L^4)]_n$ *4*

Compound $\mathbf{L^4}$ was dissolved in 5 ml of chloroform (0.05 g, 0.05 mmol), and a solution of copper(II) acetate (0.04 g, 0.20 mmol) in 5 ml of acetonitrile was added dropwise while stirring. During the addition, a green solid started to deposit. The microcrystals obtained in this manner were washed with distilled water, followed by hot hexanes, for a 73% yield of **4** (0.06 g, 0.04 mmol). Anal. calcd for $C_{84}H_{100}N_4O_{20}Cu_4$ (**4**): C 57.99, H 5.79, N 3.22. Found: C 57.98, H 5.66, N 3.38%. IR (KBr, cm^{-1}): $\nu = 3064, 2960, 2870, 1624, 1480, 1435, 1366, 1300, 1241, 1197, 1127, 1031, 870, 766, 682, 629$. UV–vis [$\lambda_{max}$, nm ($\varepsilon$, $l\,mol^{-1}\,cm^{-1}$)]: (THF solution) 671 (588).

ESR spectroscopy

ESR measurements were made in quartz tubes at room temperature with a JEOL JES-TE300 spectrometer operating at X-band frequency (near 9.4 GHz) at 100 KHz field modulation, with a cylindrical cavity (TE_{011} mode). The external measurement of the static magnetic field was made with a precision JEOL ES-FC5 gaussmeter. For low-temperature measurements, an ITC^{503} (Oxford) variable temperature controller unit was employed. Spectral acquisition and manipulations were performed using the program ESPRIT-382 v1.916.

X-ray crystallography

Data were collected on a Bruker SMART X-ray diffractometer equipped with an Apex CCD area detector with graphite-monochromated Mo-Kα radiation ($\lambda = 0.71073$ Å). Unit cell constants were obtained from the least-squares refinements of the observed reflections using the ω-scan mode. The structures were solved by direct methods and refined by full-matrix least squares on F^2 using the SHELXTL software package *(28)*. All non-hydrogen atoms were refined anisotropically, including the carbon atoms of the disordered *tert*-butyl groups commonly observed in *p-tert*-butylcalix[4]arenes, which resulted in large thermal parameters. Additionally, the THF molecules in the structure of **3** were modelled over two positions. Hydrogen atoms were placed in idealised positions, with C—H distances of 0.93 and 0.98 Å for sp^2 and sp^3 hybridised carbon atoms, respectively. The isotropic thermal parameters of the hydrogen atoms were assigned the values of $U_{iso} = 1.2$ times the displacement parameters of the corresponding C-atom to which they are attached.

Supplementary data

Crystallographic data for compounds **1** and **3** have been deposited with the Cambridge Crystallographic Data Centre, CCDC reference numbers 299054 and 299056. Copies of this information may be obtained free of charge from: The Director, CCDC, 12 Union Road, Cambridge, CB2 1EZ, UK (fax: 44 1233 336033; deposit@ccdc.cam.ac.uk or http://www.ccdc.cam.ac.uk).

Acknowledgements

The authors thank CONACYT for financial support (Proyecto 58408). JO and IC additionally thank DGAPA-UNAM (Proyectos IN2474 and IN216806).

References

(1) Gutsche, C.D. In *Calixarenes Revisited*; Stoddart, J.F., Ed.; Royal Society of Chemistry: Cambridge, 1998.
(2) Asfari, Z.; Böhmer, V.; Harrowfield, J.; Vicens, J.; Eds.; *Calixarenes 2001*; Kluwer: Dordrecht, 2001.
(3) Wieser, C.; Dieleman, C.B.; Matt, D. *Coord. Chem. Rev.* **1997**, *165*, 93–161.
(4) Sliwa, W. *J. Incl. Phenom. Macr. Chem.* **2005**, *52*, 13.
(5) Jeunesse, C.; Armspach, D.; Matt, D. *Chem. Commun.* **2005**, 5603–5614.

(6) Hosseini, M.W. *Acc. Chem. Res.* **2005**, *38*, 313–323.
(7) Blanchard, S.; Le Clainche, L.; Rager, M.-N.; Chansou, B.; Tuchagues, J.-P.; Duprat, A.F.; Le Mest, Y.; Reinaud, O. *Angew. Chem. Int. Ed.* **1998**, *37*, 2732–2735.
(8) Le Clainche, L.; Giorgi, M.; Reinaud, O. *Eur. J. Inorg. Chem.* **2000**, 1931–1933.
(9) Beer, P.D.; Martin, J. P.; Drew, M.G.B. *Tetrahedron* **1992**, *48*, 9917–9928.
(10) Eggert, J.P.W.; Harrowfield, J.M.; Lüning, U.; Skelton, B.W.; White, A.H. *Polyhedron* **2006**, *25*, 910–914.
(11) Olguín, J.; Gómez-Vidal, V.; Muñoz, E.; Toscano, R.A.; Castillo, I. *Inorg. Chem. Commun.* **2006**, *9*, 1096–1098.
(12) Creaven, B.S.; Gernon, T.L.; McCormac, T.; McGinley, J.; Moore, A.-M.; Toftlund, H. *Inorg. Chim. Acta* **2005**, *358*, 2661–2670.
(13) Iwamoto, K.; Shimizu, H.; Araki, K.; Shinkai, S. *J. Am. Chem. Soc.* **1993**, *115*, 3997–4006.
(14) Ferguson, G.; Gallagher, J.F.; Giunta, L.; Neri, P.; Pappalardo, S.; Parisi, M. *J. Org. Chem.* **1994**, *59*, 42–53.
(15) Shinkai, S.; Fujimoto, K.; Otsuka, T.; Ammon, H.L. *J. Org. Chem.* **1992**, *57*, 1516–1523.
(16) Pappalardo, S.; Giunta, L.; Foti, M.; Ferguson, G.; Gallagher, J.F.; Kaitner, B. *J. Org. Chem.* **1992**, *57*, 2611–2624.
(17) Ockwig, N.W.; Delgado-Friedrichs, O.; O'Keeffe, M.; Yaghi, O.M. *Acc. Chem. Res.* **2005**, *38*, 176–182.
(18) Nakanishi, K.; Solomon, P.H. *Infrared Absorption Spectroscopy*; Holden-Day: San Francisco, CA, 1977.
(19) Deacon, G.B.; Phillips, R.J. *Coord. Chem. Rev.* **1980**, *33*, 227–251.
(20) Cejudo, R.; Alzuet, G.; Borrás, J.; Liu-González, M.; Sanz-Ruiz, F. *Polyhedron* **2002**, *21*, 1057–1061.
(21) Wasserman, E.; Snyder, L.C.; Yager, W.A. *J. Chem. Phys.* **1964**, *41*, 1763–1772.
(22) Harish, S.P.; Sobhanadri, J. *Inorg. Chim. Acta* **1985**, *108*, 147–153.
(23) Kozlevcar, B.; Leban, I.; Turel, I.; Segedin, P.; Petric, M.; Pohleven, F.; White, A.J.P.; Williams, D.J.; Sieler, J. *Polyhedron* **1999**, *18*, 755–762.
(24) Danil de Namor, A.F.; Cleverley, R.M.; Zapata-Ormachea, M.L. *Chem. Rev.* **1998**, *98*, 2495–2525.
(25) See, for example: McKervey, M.A.; Seward, E.M.; Ferguson, G.; Ruhl, B.L. *J. Org. Chem.* **1986**, *51*, 3581–3584; Notti, A.; Occhipinti, S.; Pappalardo, S.; Parisi, M.F.; Pisagatti, I.; White, A.J.P.; Williams, D.J. *J. Org. Chem.* **2002**, *67*, 7569–7572.
(26) McIldowie, M.J.; Mocerino, M.; Ogden, M.I.; Skelton, B.W. *Tetrahedron* **2007**, *63*, 10817–10825.
(27) Dalgarno, S.J.; Thallapally, P.K.; Barbour, L.J.; Atwood, J.L. *Chem. Soc. Rev.* **2007**, *36*, 236–245.
(28) SHELXTL 6.10; Bruker Analytical Instrumentation: Madison, Wisconsin, 2000.